Ibañez C, Hernández-Figueirido D, Piquer A. Shape effect on axially loaded high strength CFST stub columns. 2018. Journal of Constructional Steel Research; 147: 247-256.
doi: 10.1016/j.jcsr.2018.04.005

Shape effect on axially loaded high strength CFST stub columns

C. Ibañez [a*], D. Hernández-Figueirido [a], A. Piquer [a]

[a] *Department of Mechanical Engineering and Construction, Universitat Jaume I, Castellón, Spain*
** Corresponding author. e-mail address: ibanezc@uji.es*

ABSTRACT

In this paper, the results of an experimental campaign on 12 concrete-filled steel tubular (CFST) stub columns subjected to concentric loads are presented. In this program, different cross-sectional shapes are considered: circular, square and rectangular. In order to study the effect of the concrete infill strength in the ultimate capacity of the columns, two types of concrete infill are employed: normal and high strength concrete of grades C30 and C90 respectively.

The specimens are classified into three different series so all the columns of a series have equivalent cross-sectional area to perform a proper comparison and draw consistent conclusions. During the tests, the response in terms of load versus column shortening is registered. In view of the experimental results, the dependency of the type of response and failure mode on the cross-sectional shape and type of infill of the columns is analysed. Besides, the influence of the concrete infill, the result of the composite action and the level of ductility are also studied.

Finally, the experimental ultimate loads of the specimens are compared with the corresponding failure loads given by the codes. In this case, comparison showed that Eurocode 4 and the Chinese and Australian standards overestimate the failure load of the specimens, particularly for square and rectangular CFST columns. The American code tends to be more conservative in its predictions for circular columns, although it is still unsafe for those with square and rectangular steel tubes.

Keywords: *composite stub columns; concrete-filled steel tubes; high strength concrete; sectional capacity; shape effect.*

NOTATION

AISC	American Institute of Steel Construction
AS	Australian Standard
CCR	Concrete contribution ratio
CFST	Concrete-filled steel tube
D	Diameter of the steel tube
DBJ	Chinese Code
DI	Ductility Index
EC4	Eurocode 4
f_c	Compressive cylinder strength (150x300 mm) of concrete (test date)
f_{ck}	Characteristic compressive strength of concrete
f_{cu}	Compressive cubic strength (150x150x150 mm) of concrete (test date)
f_y	Yield strength of structural steel
HSC	High strength concrete
NSC	Normal strength concrete
N_{exp}	Ultimate axial load from tests
N_{cr}	Euler critical load $N_{cr} = (\pi^2 EI)/L^2$
L	Column length
SI	Strength Index
t	Thickness of the steel tube
$\bar{\lambda}$	Relative slenderness $\bar{\lambda} = \sqrt{N_{pl}/N_{cr}} = \sqrt{(A_c f_c + A_s f_y)/N_{cr}}$

δ Axial displacement at maximum load

$\delta_{85\%}$ Axial displacement at 85% of the maximum load at the decay branch

ρ Concrete density

Ibañez C, Hernández-Figueirido D, Piquer A. Shape effect on axially loaded high strength CFST stub columns. 2018. Journal of Constructional Steel Research; 147: 247-256.
doi: 10.1016/j.jcsr.2018.04.005

1. INTRODUCTION

The use of concrete-filled steel tubes (CFST) as composite columns is widely extended around the world. Their high bearing capacity with reduced sections, large energy absorption in case of seismic, rapid erection times or ease of construction are some of the advantageous characteristics that have made CFST successful over traditional columns [1]. In general, it was found out that the enhancement in the mechanical response of these columns is due to the composite action between the hollow steel tube and the concrete core. The concrete core is confined by the steel tube which increases the compressive strength of the section and its ductility. In turn, the concrete infill prevents the steel tube from local buckling, especially in rectangular CFST with thin-walled steel tubes. However, this effect is influenced by the cross-sectional aspect ratio, the strength of the materials and the confining factor, highly dependent of the cross-sectional shape [2].

The behaviour of CFST stub columns under axial compression over different cross-sectional shapes have been investigated by several authors through various experimental programs (Schneider [2], Han [3], Giakoumelis and Lam [4], Lam and Williams [5], Sakino et al. [6], Tao et al. [7], Han et al. [8], Ellobody et al. [9], Liang and Fragomeni [10], Tahyalan et al. [11], Ekmekyapar and Al-Eliwi [12]). Most of them focused on the use of normal strength concrete (NSC), but, more recently, also high strength concrete (HSC) has been included.

Currently, although the performance of special-shaped CFST columns under axial compression is starting to be investigated (Ren et al.[13], Ding et al. [14], Xu et al. [15]), the most employed shapes are still circular, square or rectangular CFST columns. Confinement in circular sections is enhanced due to the hoop stresses appearing because of the composite action. However, the advantageous effect on the confinement when high strength concrete (HSC) is employed is not well established, especially for thin-walled steel tubes.

Given the structural benefits of CFST columns and their high load bearing capacity they are commonly employed in high rise buildings, heavy loaded structures or underground structures. As the required column loading capacity increases, the dimensions of the CFST column also become larger. As pointed out by Wang et al. [16], the size effect is enhanced in plain concrete for higher values of D/t and leads to a reduction of the hoop stresses in the steel tube which, in turn, leads to a reduction of the confinement effect. For these members with large dimensions, the adoption of HSC can significantly reduce the column size and permits to achieve higher strength to weight ratio still maintaining a reasonable level of ductility. The beneficial application of HSC in the building industry makes interesting its study, particularly when employed in CFST columns.

Together with the investigations on the behaviour of CFST columns, many design codes have been extended or created in order to try to cover the structural applications of these composite sections and give design and calculation guidance. Nevertheless, the application of the methods included in the codes is still limited to a certain range of material strengths, geometries and cross-sectional slenderness. Some investigations can be found dealing with the assessment of the existing codes for predicting the ultimate strength of CFST stub columns [3][4][7][12][17]. For columns whose characteristics are within the limits, comparisons of the strength predictions given by the codes with experimental results sometimes are not completely satisfactory, either overpredicting or underpredicting the ultimate strength of the columns. Applying the current code provisions to any other CFST column out of the applicability range will produce less accurate strength predictions.

At present, some examples of structures designed and built with high strength CFST columns can be found. As pointed out by Wang et al. [17], this fact evidences the imminent normalization of the use of these composite sections and confirms the necessity of developing reliable design methods which consider high performance materials.

In the view of the analysis of the literature, it is detected a lack of experimental tests on CFST columns with HSC to completely understand its effect on this type of composite members. Therefore, a new experimental program on stub CFST columns was designed where specimens with circular, square and rectangular cross-sections were tested. The experiments combined the use of NSC and HSC to study their effect on the load bearing capacity of columns with different shape subjected to concentric loads.

Finally, the specifications of current codes for the design of CFST columns are assessed. In this comparison, four commonly used codes are considered: European code Eurocode 4 (EC4) [18], American code (AISC) [19], Chinese code (DBJ) [20], and the Australian code (AS) [21].

2. EXPERIMENTAL INVESTIGATION

2.1. Column specimens and test setup

In this work, a total of 12 CFST stub columns were tested with the objective of evaluating the effect of the concrete infill strength and cross-sectional shape on their load bearing capacity. Three different series were distinguished depending of the amount of steel area of the steel tubes. For each series, the compressive strength of the concrete poured inside the steel tubes varied between C30 and C90. Besides, different cross-sectional shapes were compared: circular (C), rectangular (R) and square (S) as shown in Fig. 1.

It is important to note that this experimental program was designed to assure that all the specimens of a series had the same steel cross-sectional area so as this parameter did not affect the conclusions drawn from the shape effect analysis. In Table 1, cross-sectional properties of all test specimens and other data corresponding to each series are summarized. For convenience, the test specimens were named as follows: S-D_N (i.e. C159x3_30), where S stands for the cross-sectional shape of the steel tube (C for circular steel tubes, R for rectangular and S for square); D represent the cross-sectional dimensions in mm; and N is the nominal concrete strength in MPa.

All the columns were manufactured and tested at the Universitat Jaume I in Castellón (Spain) in a horizontal testing frame with capacity of 5000 kN. Fig. 2 and Fig. 3 show some of the specimens prior to be tested and the setup of one of the experiments respectively. During the tests, all the columns had a buckling length of 300 mm with pinned-pinned (P-P) boundary conditions. For the sake of accuracy of the measurements, the corresponding displacement control test was performed after the correct collocation of the column.

2.2. Material properties

Steel tubes

In this experimental program, all steel tubes were cold-formed carbon steel and supplied by the same manufacturer. The nominal yield strength of the tubes varied between S355 and S275. In order to provide enough material for the coupon tests, the total length of the tubes supplied was more than that strictly needed for the CFST columns. Therefore, from the extra length of the tubes the coupon tests were obtained. For all the hollow steel tubes employed, the actual values of the yield strength (f_y) were determined through the corresponding coupon tests (3 tests per tube) and are shown in Table 1. According to the European standards, the modulus of elasticity of steel was set to 210 GPa.

Concrete

As exposed above, two grades of nominal compressive strength were employed: C30 and C90, whose mix proportions are summarized in Table 2 for each batch respectively. In this program, only commercially available materials were employed. A planetary mixer was employed to prepare the mixings. Together with the experiment on the stub column, the corresponding tests were carried out on the 150x300 mm cylinders in order to obtain the actual compressive strength (f_c) which characterizes each concrete infill of the column as shown in Table 1. For that task, sets of concrete samples were prepared and cured in standard conditions during 28 days until the day when the test was performed. Concrete was placed in the corresponding steel tubes and cylinder molds in several layers and each layer was compacted by means of a vibrator rod. Later, the CFST columns were covered with wet clothes and let to cure. Before the test of the concrete samples, their end surfaces were treated and prepared to ensure the simultaneous loading of both components.

3. TEST PROCEDURE AND RESULTS

3.1. Test procedure

Firstly, the specimens were placed horizontally in the testing frame (Fig. 3) and correctly positioned in order to ensure that uniquely pure compression was applied to the columns. Once the specimens were put in place, the test started using a displacement control protocol to properly register the post-peak response of the stub columns. The displacement was imposed to a very slow rate so that local buckling of the CFST columns could be observed in detail. The specimens were tested to failure under axial compression and after the peak load was achieved, the test was continued at least until the load reached back the 85% of its peak load in order to obtain enough experimental data for the posterior analysis. The response of most of the specimens was relatively ductile so the experiments were performed in a gentle and controlled way. When the experiment ended, the stub column was removed and kept for being examined.

3.2. Maximum load

As expected, it was found that the typical failure mode for the tested specimens was crushing of concrete with local buckling (outwards folding) of the steel tube close to the ends of the column. Fig. 4 shows one of the stub columns with square cross-section after the test.

During the tests, the response of the columns was registered in terms of the variation of the load along with the shortening of the column. In Fig. 5 these curves are plotted for the three different series. Besides, for each specimen, the value of the ultimate load was obtained and plotted in Fig. 6. In Table 1 these values have been summarized.

Regarding the shape effect, it can be seen that for those columns with equivalent steel area, the experimental loads obtained for circular CFST columns are higher than for square or rectangular sections. It can also be noticed that even with less steel area, circular CFST

columns of series 2 are able to achieve higher loads than square or rectangular columns from series 1.

It can be observed in Fig. 6.that, as expected, the concrete strength has a positive effect on the ultimate capacity of the columns and those with HSC show higher maximum loads. However, although all the specimens have similarities regarding the failure mode, the effect of using various types of concrete is reflected in the different form of the compression load-shortening curves. Those columns with HSC show in general a very different behaviour compared to NSC columns. For HSC columns, the change from the pre-peak to the post-peak is very sharp in contrast to the smooth transition observed in NSC specimens. This behaviour can be explained by the brittle nature of HSC and implies that the steel tube of the column is not able to produce the same amount of confinement that in the case of columns filled with NSC concrete.

For each series, formed by columns which have an equivalent steel area, it has been confirmed that the ultimate capacity of those with higher areas of concrete is enhanced. This is due to the type of test carried out, since concrete has its optimal performance under pure compression.

3.3. Strength Index

The strength index (SI) is the ratio between the theoretical cross-sectional capacity and the actual ultimate load. It helps to measure the synergy existing between the two components (steel tube and concrete core) of the CFST column. It was calculated for each column by means of:

$$SI = \frac{N_{\exp}}{A_s f_y + A_c f_c} \tag{1}$$

where N_{exp} is the experimental ultimate load, A_s is the cross-sectional area of the steel tube, f_y is the yield strength of the steel tube, A_c is the concrete cross-sectional area and f_c the

concrete strength. This parameter is calculated for all the columns and the values are summarized in Table 1 and plotted in Fig. 7 for each series.

In view of the results, it can be observed that for NSC only those CFST columns with circular steel tubes show values of SI higher than one. This is due to the effect of the confinement which leads to cross-sectional capacities higher than the sum of all the components. For square and rectangular specimens, the load-bearing capacity is not improved in any case which means that the sectional capacity calculated as the sum of all the components overestimate the ultimate load of the members.

Regarding columns with HSC, the value of SI is in general less than one. These low values of SI corroborate the trend observed in the previous analysis resulting in a less effective confinement when HSC is employed.

3.4. Concrete Contribution Ratio (CCR)

In a similar way, the contribution of the concrete infill was analysed for each member by means of the concrete contribution ratio which is given by:

$$CCR = \frac{N_{\exp}}{A_{s,eff}\, f_y} \tag{2}$$

where N_{exp} is the experimental ultimate load, $A_{s,eff}$ is the effective cross-sectional area of the steel tube according to the Eurocode 3 model [22], that considers the local buckling of the steel hollow tube and f_y is the yield strength of the steel tube.

In Fig. 8, the values of CCR are plotted for the three series of the campaign and also are included in Table 1. The results obtained support the tendency observed for the experimental ultimate loads. The effect of the concrete infill is much higher when HSC is employed and, again, it is more effective to fill circular steel tubes than those with rectangular or square sections.

3.5. Ductility Index (DI)

The last parameter employed for the analysis of the experimental results is the ductility index (DI) which is based on the load-axial shortening curves. In this paper, the definition proposed by Tao et al. [23] is adopted as suggested by other authors [3]. DI is calculated as the inverse ratio between the axial shortening of the CFST column corresponding to the peak load (N_{exp}) and the axial shortening of the column corresponding to the point when it reaches back the 85% of the peak load (N_{exp}) in the decay branch. The higher the value of DI, the higher the ductility of the CFST columns since it implies that the slope of the decay branch of the load-shortening curve is smooth. It is obtained by:

$$DI = \frac{\delta_{85\%}}{\delta} \tag{3}$$

where δ is the axial shortening of the stub column corresponding to the peak load and $\delta_{85\%}$ is the axial shortening of the column when the load has fallen to the 85% of the peak load.

Also the values of the DI for the columns tested are summarized in Table 1 and the comparison for the three series can be seen in Fig. 9. Due to the particularly long duration of two of the tests with NSC and the specifications of the equipment employed, the experiments were stopped before the stub column reached back the 85% of the peak load. Therefore, the DI cannot be calculated in these two cases, but this fact is a clear proof of the high ductility of these two columns (Columns C100x3_30 and C101.6x3_30 from series 3) as can be seen in Fig. 6.

As expected, those columns with NSC showed higher values of DI than those with HSC whose DI values are close to one. This is in concordance with the abrupt transition from the pre-peak to the post-peak region in the load-shortening curves.

4. COMPARISON OF RESULTS WITH CODE PREDICTIONS

In this section, the design approaches adopted in European code Eurocode 4 EN1994-1-1 (EC4) [18], American code (AISC) [19], Chinese code DBJ 13-51-2010 (DBJ) [20] and the Australian code AS5100 (AS) [21] are commented and applied to calculate the ultimate strength of the tests columns. Subsequently, the predicted values are compared with the experimental results obtained from the experiments.

A brief review of the methods of the current codes for the prediction of the axial capacity of circular and rectangular stub columns as well as their limitations are presented in Table 4. In this work, for all the design calculations, the resistance factors and material factors are set to one.

Design codes consider different expressions for the sectional capacity (squash load) of CFST columns. However, they are all based on the sum of the contributions of concrete and steel to column resistance. The lateral confinement of the concrete core is taken into account in some cases, depending on the material, the shape, the column slenderness and the relation of the thickness to the maximum dimension of the section.

In order to analyze the predictions given by the different codes, a comparative study is performed taking as references the experimental capacities obtained in the tests. Table 3 and Fig. 10 summarized the results of the analysis both numerically and graphically respectively. The error of predicting the axial capacity of the column is calculated as follow:

$$\xi = \frac{N_{\text{exp}}}{N_{\text{code}}} \tag{4}$$

where N_{exp} is the experimental ultimate capacity and N_{code} is the sectional capacity predicted by the corresponding code.

4.1.1. Eurocode 4 (EC4)

The experimental ultimate loads were compared to the maximum load calculated according to the design method proposed by Eurocode 4 (EC4) [18] for composite members. As can be seen in Table 4, the EC4 uses a different model in function of the cross-sectional shape. For rectangular sections, the capacity of the stub column is obtained as the sum of the contribution of each material. However, in the case of circular sections, for concentric axial load and relative slenderness under 0.50, the concrete contribution is enhanced and the steel capacity reduced.

The results obtained by this method are summarized in Table 3 (N_{EC4}) together with the error calculated with respect to the experimental values. As can be seen in Fig. 10a, EC4 produces in general unsafe predictions with a mean of 0.86, and it is especially unsafe for those specimens with square or rectangular cross-sections.

4.1.2. American Institute of Steel Construction (AISC)

In the same line, the AISC [19] composite column design presents different equations for the cross sectional strength depending on the shape of the column and the ratio maximum dimension to thickness. As summarized in Table 4, in this case, the code considers high strength concrete ($fc \leq 70$ MPa) and allows an increase of concrete stress in case of circular sections due to confinement. Besides, the expression for the nominal axial capacity of stub columns incorporates the effect of slenderness.

In Table 3, the predictions given by this method are presented (N_{ASIC}) and also the error obtained with respect to the tests values. The graphical representation of this data is displayed in Fig. 10b where it can be seen that for circular columns of both NSC and HSC, AISC produces safer results than EC4 with a mean of 1.02. In the same line, is less conservative for square and rectangular specimens.

4.1.3. Chinese standard (DBJ13-51:2010)

The Chinese standard code [20] bases its approach in the definition of an equivalent material for the composite section in order to simplify the design method, see Table 4. This code also considers high strength concrete and the influence of the maximum dimension to thickness ratio.

The predictions given by this method are shown in Table 3 and Fig. 10c (N_{DBJ}) and are in general unsafe, particularly for square and rectangular columns. They produce an unsafe mean with the lowest value (0.82) of all the methods analysed.

4.1.4. Australian Standard (AS5100)

The Australian Standard [21] presents a model which is similar to that proposed by EC4, where the capacity of square and rectangular columns is obtained by the sum of the individual capacities of the materials and for circular columns, the model includes the confinement effect of the steel tube to the concrete core (for concentric loads and slenderness not greater than 0.5).

Due to that fact, the values of the predicted capacities given by this method are practically the same than those calculated by EC4. In general, a tendency to produce unsafe results (mean error 0.87) is observed, although for circular columns the maximum error is inside the -15% boundary. In the case of specimens with square and rectangular sections, the results are more unsafe.

5. SUMMARY AND CONCLUSIONS

The results of an experimental campaign on 12 concrete-filled steel tubular (CFST) stub columns subjected to concentric loads are presented in this paper. Different cross-sectional shapes were considered as well as two types of concrete infill (NSC and HSC). Three different series consisting of specimens with different shape but equivalent cross-sectional

steel area were designed to perform a proper analysis. From the tests, the response in terms of load versus column shortening was obtained. Based on the experimental results, several parameters were used for the analysis of the influence of the concrete infill, the composite action and the level of ductility. Finally, the experimental ultimate loads were compared with the corresponding code predictions. Several aspects from this study are worth noting:

- The typical failure was crushing of concrete with local buckling. Circular columns showed higher ultimate capacities than those with rectangular cross-sections and equivalent steel area.
- CFST columns with HSC had the highest maximum loads. CCR values proved the high efficiency of using HSC as infill, especially in circular steel tubes.
- SI values showed the important effect of confinement in circular columns filled with NSC. For rectangular columns, the positive effect of the confinement is not observed and the theoretical sectional capacity overestimated the real capacity.
- As expected, a more ductile response was observed for columns with NSC expressed in the load-shortening curve with a smooth decay branch. Contrarily, DI values for HSC are lower, corresponding to a curve with an abrupt transition.
- EC4, DBJ and AS standards overestimate the failure load of the specimens, particularly for square and rectangular CFST columns. The AISC is safer for circular columns, but still unsafe for square and rectangular specimens. Thus, in view of the results, it can be stated that further tests are needed for evaluating the actual accuracy of the different codes on predicting the capacity of stub CFST columns with different shapes and concrete grade infills.

ACKNOWLEDGEMENTS

The authors would like to express their sincere gratitude to the Generalitat Valenciana for the project (GV/2015/098), entitled “Análisis numérico de la configuración óptima y sostenible de pilares mixtos tipo concrete filled steel tubes (CFT)”).

REFERENCES

[1] Zhao XL, Han LH, Lu H. "Concrete-filled tubular members", 1st Ed. Oxon: Spon Press; 2010.

[2] Schneider SP. Axially loaded concrete-filled steel tubes. Journal of Structural Engineering 1998; 124(10): 1125-1138.

[3] Han LH. Tests on stub columns of concrete-filled RHS sections. Journal of Constructional Steel Research 2002; 58 (3):353-372.

[4] Giakoumelis G, Lam D. Axial capacity of circular concrete-filled tube columns. Journal of Constructional Steel Research 2004; 60: 1049-1068.

[5] Lam D, Williams CA. Experimental study on concrete filled square hollow sections. Steel and Composite Structures 2004; 4 (2):95-112.

[6] Sakino K, Nakahara H, Morino S, Nishiyama I. Behavior of centrally loaded concrete-filled steel-tube short columns. Journal of Structural Engineering 2004; 130(2): 180-188.

[7] Tao Z, Han LH, Wang ZB. Experimental behaviour of stiffened concrete-filled thin-walled hollow steel structural (HSS) stub columns. Journal of Constructional Steel Research 2005; 61: 962-983.

[8] Han LH, Yao GH, Zhao XL. Tests and calculations for hollow structural steel (HSS) stub columns filled with self-consolidating concrete (SCC). Journal of Constructional Steel Research 2005; 61(9): 1241-1269.

[9] Ellobody E, Young B, Lam D. Behaviour of normal and high strength concrete-filled compact steel tube circular stub columns. Journal of Constructional Steel Research 2006; 62(7): 706-715.

[10] Liang QQ, Fragomeni S. Nonlinear analysis of circular concrete-filled steel tubular short columns under axial loading. Journal of Constructional Steel Research 2009; 65(12): 2186-2196.

[11] Thayalan P, Aly T, Patnaikuni I. Behaviour of concrete-filled steel tubes under static and variable repeated loading. Journal of Constructional Steel Research 2009; 65(4):900-908.

[12] Ekmekyapar T, Al-Eliwi B. Experimental behaviour of circular concrete filled steel tube columns and design specifications. Thin-Walled Structures 2016; 105: 220-230.

[13] Ren QX, Han LH, Lam D, Hou C. Experiments on special-shaped CFST stub columns under axial compression. Journal of Constructional Steel Research 2014; 98(7):123-133.

[14] Ding F, Li Z, Cheng S, Yu Z. Composite action of octagonal concrete-filled steel tubular stub columns under axial loading. Thin-Walled Structures 2016; 107: 453-461.

[15] Xu W, Han LH, Li W. Performance of hexagonal CFST member under axial compression and bending. Journal of Constructional Steel Research 2016; 123: 162-175.

[16] Wang W, Ma H, Li Z, Tang Z. Size effect in circular concrete-filled steel tubes with different diameter-to-thickness ratios under axial compression. Engineering Structures 2017; 151: 554-567.

[17] Wang ZB, Tao Z, Han LH, Uy B, Lam D, Kang WH. Strength, stiffness and ductility of concrete-filled steel columns under axial compression. Engineering Structures, 2017; 135: 209-221.

[18] CEN EN 1994-1-1. Eurocode 4: Design of composite steel and concrete structures. Part 1-1: General rules and rules for buildings. Brussels, Belgium: Comité Européen de Normalisation; 2004

[19] AISC-360-10: Specification for Structural Steel Buildings. Chicago, USA. American Institute of Steel Construction, 2010.

[20] DBJ13-51-2010: Technical specification for concrete-filled steel tubular structures. Fuzhou, China. The Construction Department of Fujian Province, 2010.

[21] AS5100: Bridge design-steel and composite construction. Australian Standard, 2004.

[22] CEN EN 1993-1-1. Eurocode 3: Design of steel structures. Part 1.1: General rules and rules for buildings. Brussels, Belgium: Comité Européen de Normalisation; 2005.

[23] Tao Z, Han LH, Zhao XL. Behaviour of square concrete filled steel tubes subjected to axial compression. Proceedings of the Fifth International Conference on Structural Engineering for Young experts, China, 1998; 61-67.

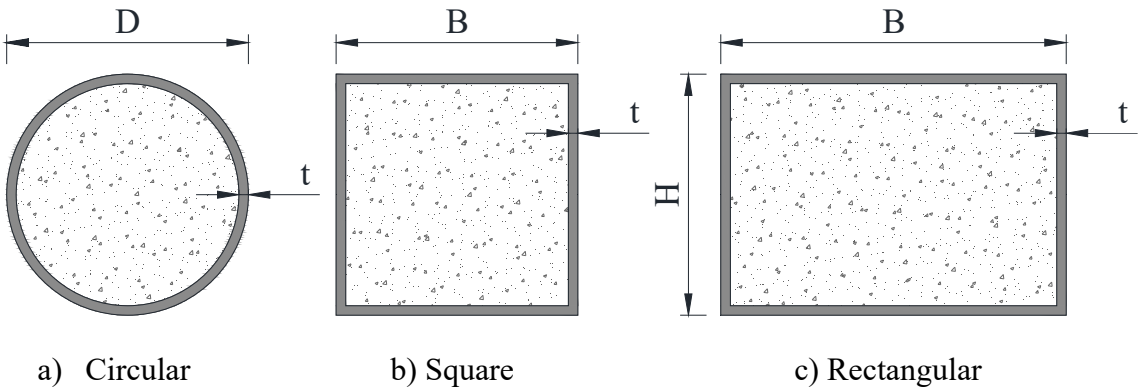

Fig. 1. CFST sections: a) Circular b) Square c) Rectangular

Fig. 2. Specimens ready to be tested

a)

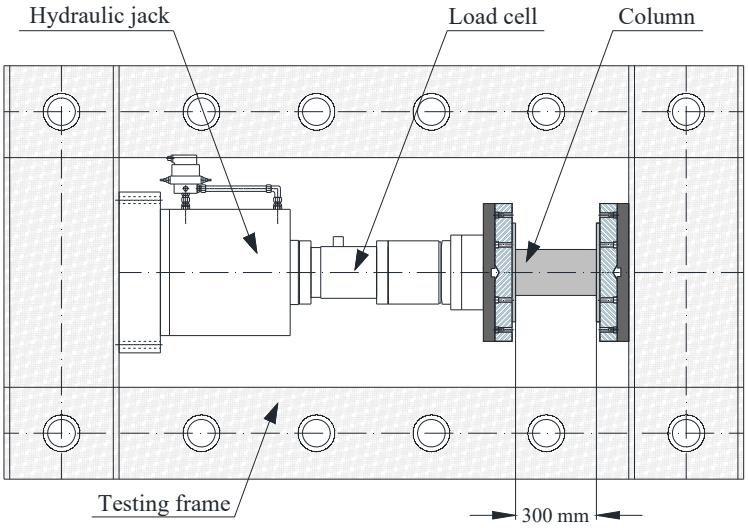

b)

Fig. 3. a) General scheme of the test setup b) Detail of the test setup for one of the specimens

Fig. 4. Typical failure mode (S125x125x3_30)

a)

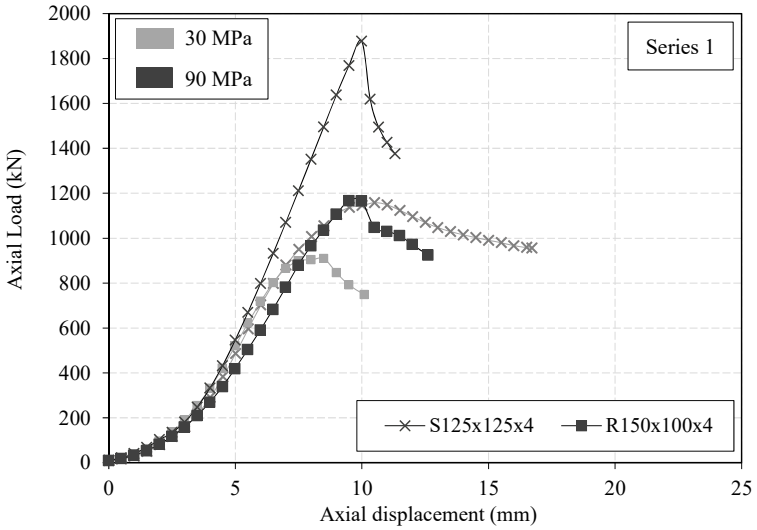

b)

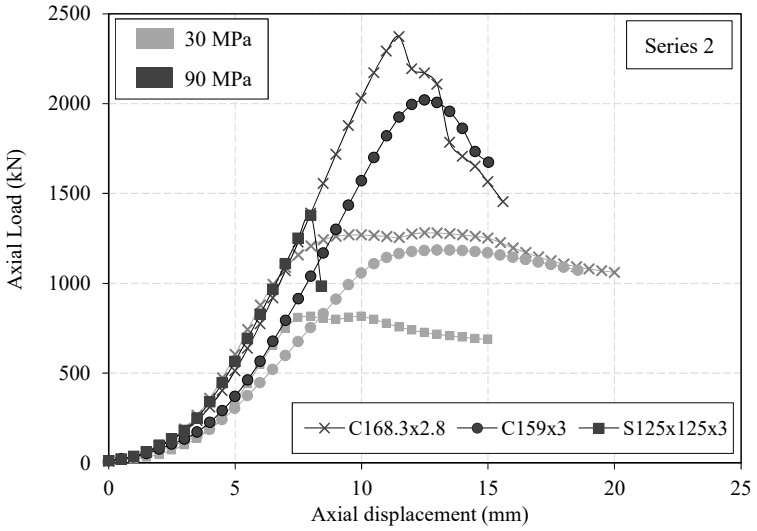

c)

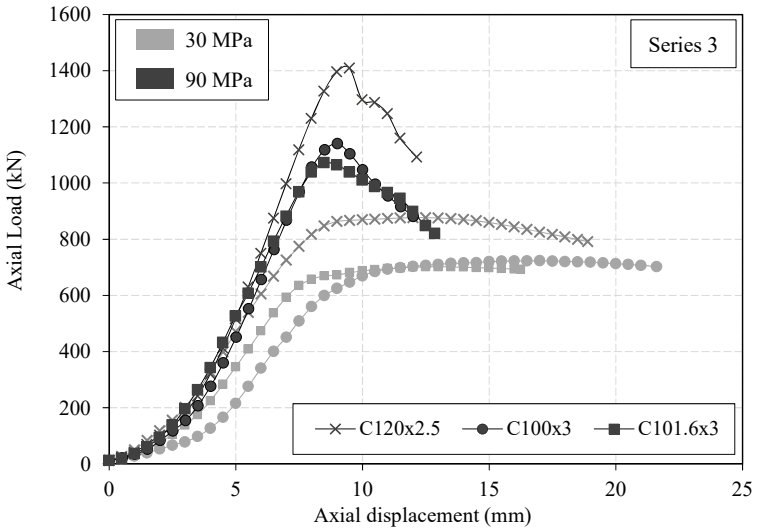

Fig. 5. Compression load versus shortening for: a) Series 1, b) Series 2, c) Series 3.

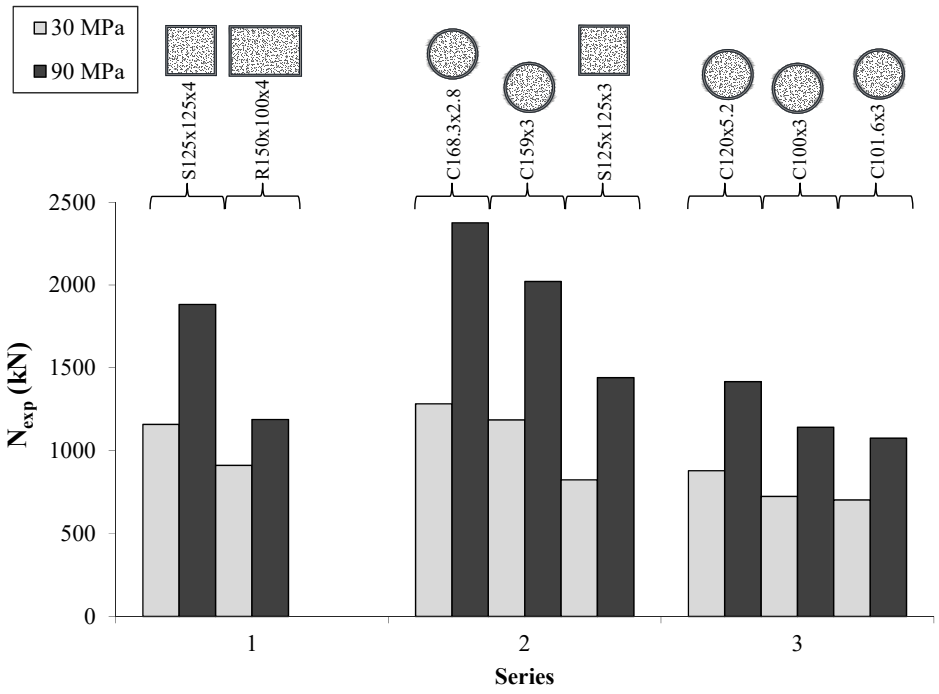

Fig. 6. Maximum load (N_{exp})

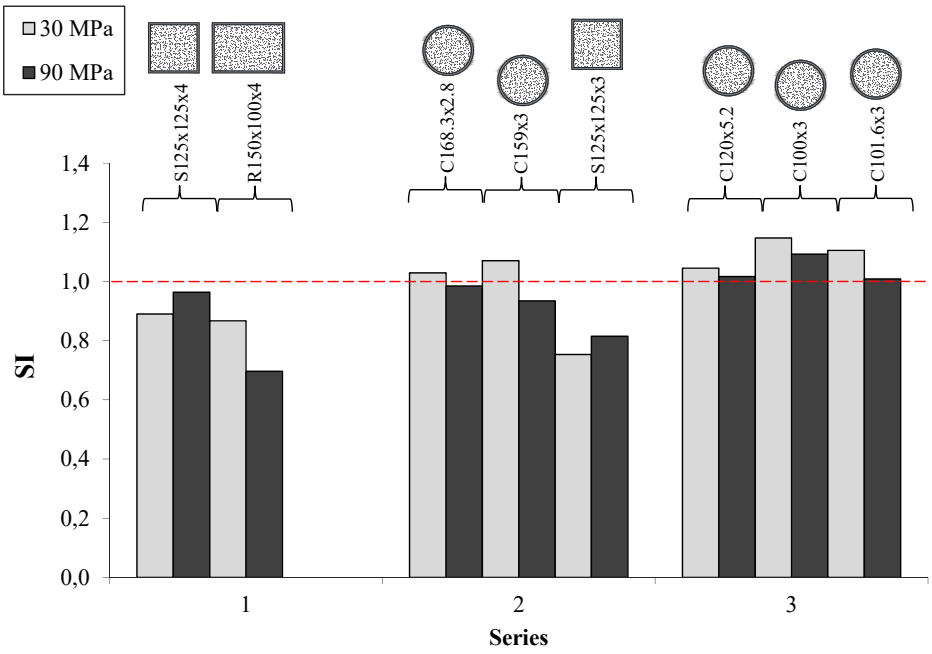

Fig. 7. Strength index (SI)

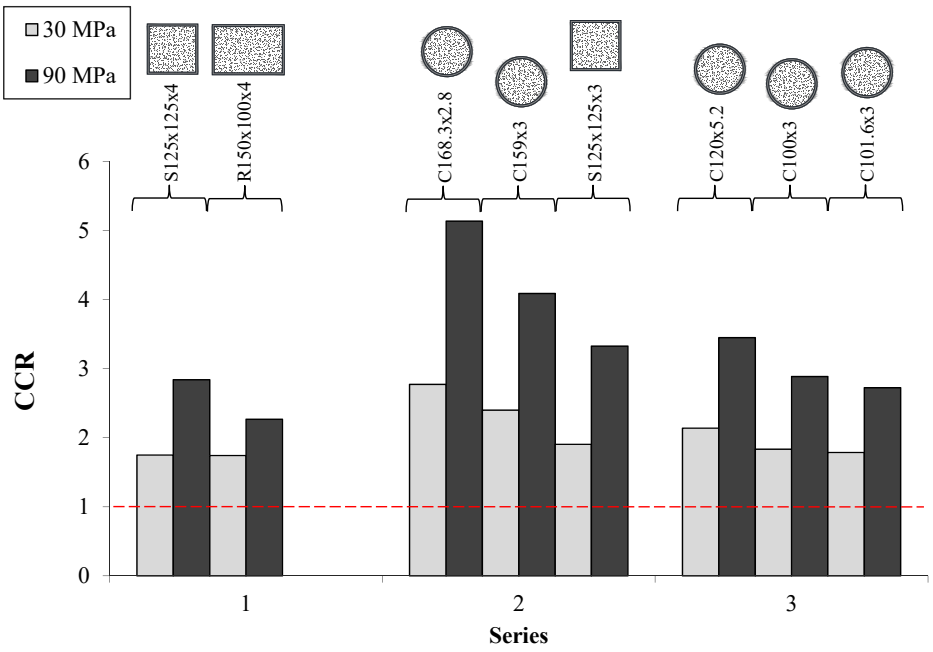

Fig. 8. Concrete contribution ratio (CCR)

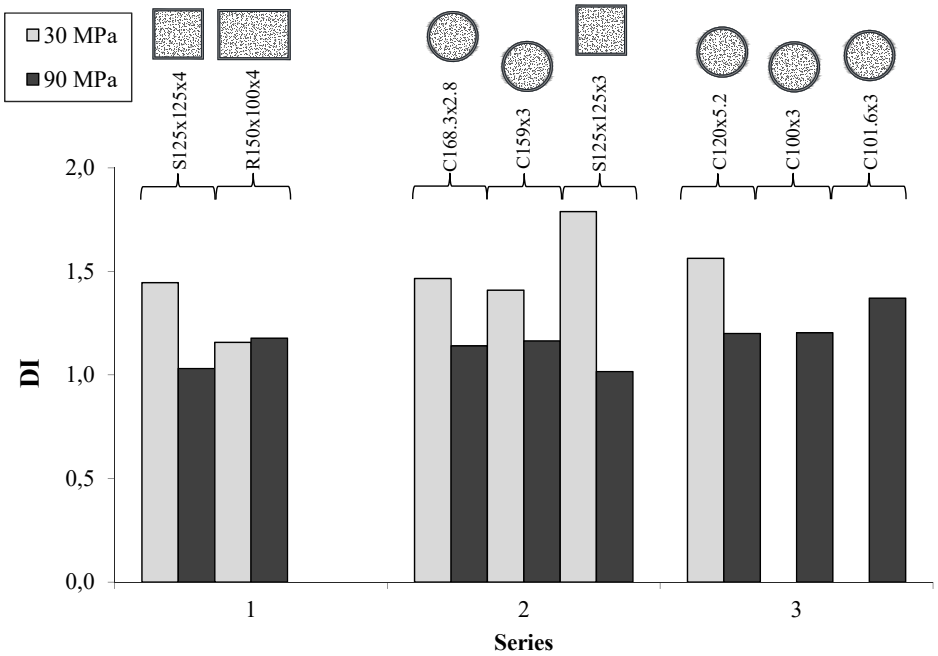

Fig. 9. Ductility index (DI)

Ibañez C, Hernández-Figueirido D, Piquer A. Shape effect on axially loaded high strength CFST stub columns. 2018. Journal of Constructional Steel Research; 147: 247-256.
doi: 10.1016/j.jcsr.2018.04.005

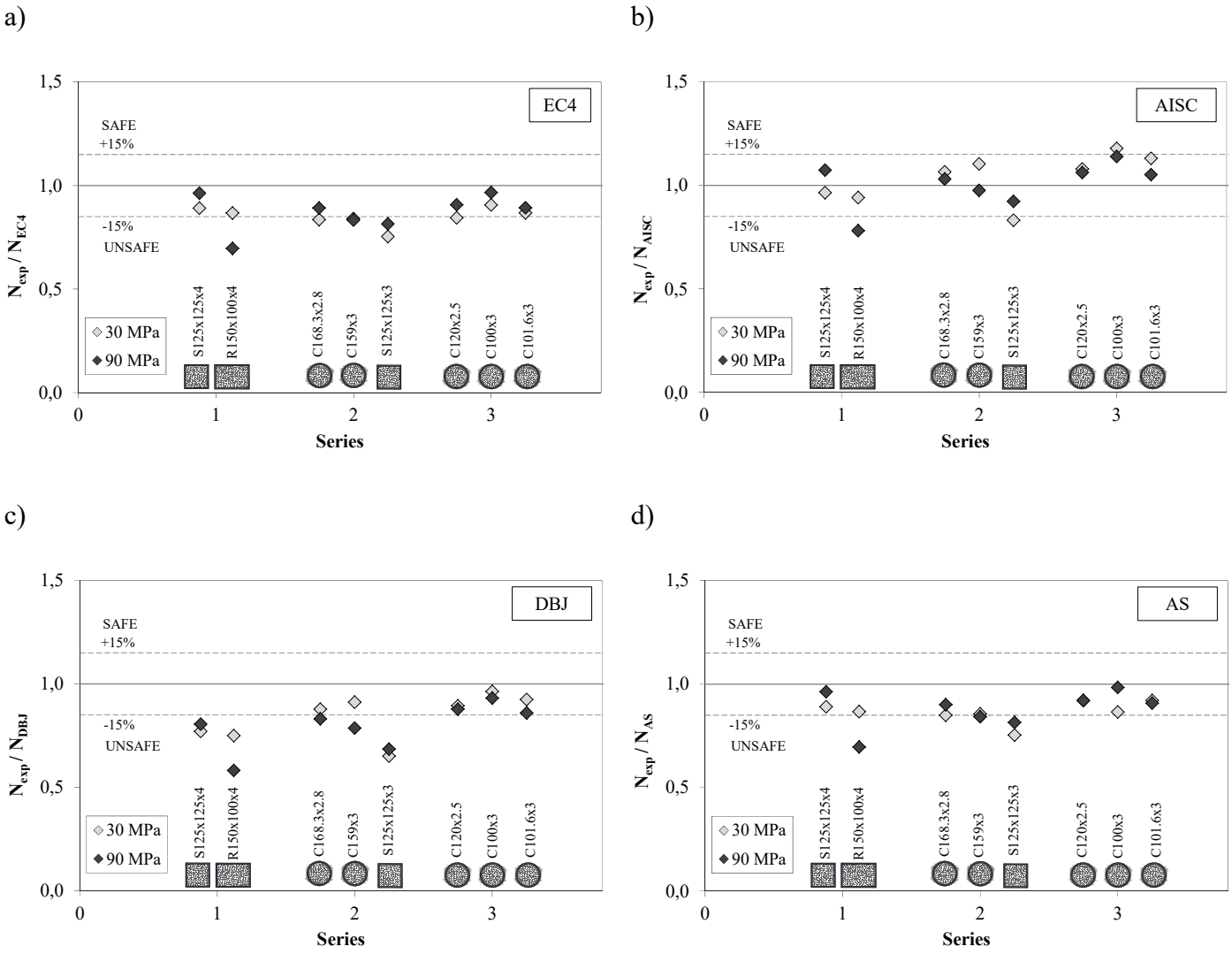

Fig. 10. Comparison between the predicted and measured cross-sectional strength.

Ibañez C, Hernández-Figueirido D, Piquer A. Shape effect on axially loaded high strength CFST stub columns. 2018. Journal of Constructional Steel Research; 147: 247-256.
doi: 10.1016/j.jcsr.2018.04.005

Table 1. Details of the column specimens and test results

Series	Name	Dimensions (mm)	t (mm)	A_s (mm^2)	f_y (MPa)	f_c (MPa)	N_{exp} (kN)	δ (mm)	$\delta_{85\%}$ (mm)	SI	CCR	DI
1	S125x125x4_30	125x125	4	1936	342,59	46.67	1159.2	10.49	15.16	0.89	1.75	1.45
	S125x125x4_90	125x125	4	1936	342.59	94.33	1882.5	10.04	10.35	0.96	2.84	1.03
	R150x100x4_30	150x100	4	1936	270.84	40.41	912	8.34	9.65	0.87	1.74	1.16
	R150x100x4_90	150x100	4	1936	270.84	90.58	1188.5	9.77	11.51	0.70	2.27	1.18
2	C168.3x2.8_30	168.3	2.8	1456	317.8	37.71	1282.5	12.66	18.56	1.03	2.77	1.47
	C168.3x2.8_90	168.3	2.8	1456	317.8	93.74	2375.7	11.57	13.2	0.99	5.14	1.14
	C159x3_30	159	3	1470	336.28	33.39	1185.7	13.17	18.56	1.07	2.40	1.41
	C159x3_90	159	3	1470	336.28	90.85	2021.7	12.53	14.58	0.93	4.09	1.16
	S125x125x3_30	125x125	3	1464	296.06	46.67	824.5	7.79	13.93	0.75	1.90	1.79
	S125x125x3_90	125x125	3	1464	296.06	94.31	1441.2	8.33	8.46	0.81	3.33	1.02
3	C120x2.5_30	120	2.5	923	445.52	41.44	879.2	12.09	18.90	1.04	2.14	1.56
	C120x2.5_90	120	2.5	923	445.52	94.68	1417.2	9.34	11.21	1.02	3.45	1.20
	C100x3_30	100	3	914	432.09	34.04	724	16.42	_	1.15	1.83	_
	C100x3_90	100	3	914	432.82	93.51	1141.3	8.98	10.81	1.09	2.88	1.20
	C101.6x3_30	101.6	3	929	425.03	34.04	703.3	13.39	_	1.10	1.78	_
	C101.6x3_90	101.6	3	929	425.03	93.51	1075.5	8.65	11.86	1.01	2.72	1.37

Table 2. Concrete mix proportions

Type of infill	C30	C90
Cement (kg/m^3)	348	570
Water (l/m^3)	220	180
Sand (kg/m^3)	1065	705
Gravel (kg/m^3)	666	890
Silica fume (kg/m^3)	-	50
Superplasticizer (kg/m^3)	-	12.3

Ibañez C, Hernández-Figueirido D, Piquer A. Shape effect on axially loaded high strength CFST stub columns. 2018. Journal of Constructional Steel Research; 147: 247-256.
doi: 10.1016/j.jcsr.2018.04.005

Table 3. Experimental and predicted cross-sectional strength

Series	Name	N_{exp} (kN)	EC4		AISC		DBJ		AS	
			N_{EC4} (kN)	N_{exp}/N_{EC4}	N_{AISC} (kN)	N_{exp}/N_{AISC}	N_{DBJ} (kN)	N_{exp}/N_{DBJ}	N_{AS} (kN)	N_{exp}/N_{AS}
1	S125x125x4_30	1159.2	1302.12	0.89	1202.26	0.96	1503.98	0.77	1302.12	0.89
	S125x125x4_90	1882.5	1954.54	0.96	1753.63	1.07	2335.71	0.81	1954.54	0.96
	R150x100x4_30	912	1052.26	0.87	969.05	0.94	1216.77	0.75	1052.26	0.87
	R150x100x4_90	1188.5	1707.68	0.70	1521.79	0.78	2041.44	0.58	1707.68	0.70
2	C168.3x2.8_30	1282.5	1535.53	0.84	1204.22	1.07	1461.28	0.88	1510.47	0.85
	C168.3x2.8_90	2375.7	2663.58	0.89	2305.21	1.03	2857.56	0.83	2638.96	0.90
	C159x3_30	1185.7	1410.53	0.84	1074.53	1.10	1300.40	0.91	1385.05	0.86
	C159x3_90	2021.7	2426.29	0.83	2072.60	0.98	2570.43	0.79	2400.83	0.84
	S125x125x3_30	824.5	1094.33	0.75	991.92	0.83	1266.98	0.65	1094.33	0.75
	S125x125x3_90	1441.2	1768.96	0.81	1562.00	0.92	2104.33	0.68	1768.96	0.81
3	C120x2.5_30	879.2	1042.00	0.84	815.10	1.08	983.06	0.89	1016.85	0.86
	C120x2.5_90	1417.2	1563.14	0.91	1334.97	1.06	1615.06	0.88	1539.51	0.92
	C100x3_30	724	799.22	0.91	614.62	1.18	751.17	0.96	777.98	0.93
	C100x3_90	1141.3	1180.56	0.97	1001.94	1.14	1224.62	0.93	1159.97	0.98
	C101.6x3_30	703.3	810.57	0.87	622.41	1.13	760.54	0.92	789.39	0.89
	C101.6x3_90	1075.5	1204.95	0.89	1022.55	1.05	1250.91	0.86	1184.39	0.91
			Mean	0.86	Mean	1.02	Mean	0.82	Mean	0.87
			SD	0.07	SD	0.11	SD	0.11	SD	0.07

Ibañez C, Hernández-Figueirido D, Piquer A. Shape effect on axially loaded high strength CFST stub columns. 2018. Journal of Constructional Steel Research; 147: 247-256.
doi: 10.1016/j.jcsr.2018.04.005

Table 4. Codes prediction methods and limitations

	Materials		Local buckling		Prediction of ultimate capacity	
	Steel f_y (MPa)	Concrete f_{ck} (MPa)	Circular	Rectangular	Circular	Rectangular
EC4 [18]	$235 \le f_y \le 460$ $E_a = 210GPa$	$25 \le f_{ck} \le 50$ $E_c = 22000\left(\frac{f_{ck}}{10}\right)^{0.3}$	$\frac{D}{t} \le 90\varepsilon^2$	$\frac{H}{t} \le 52\varepsilon$	$N_{EC4} = \eta_a A_s f_y + \left(1 + \eta_c \frac{t}{D}\frac{f_y}{f_{ck}}\right) A_c f_{ck}$	$N_{EC4} = A_s f_y + A_c f_{ck}$
AISC [19]	$f_y \le 525$ $E_a = 200GPa$	$21 \le f_{ck} \le 70$ $E_c = 0.043\rho^{1.5}\sqrt{f_{ck}}$	$\lambda_p = 0.15\frac{E_a}{f_y}$ $\lambda_p = 127.66\varepsilon^2$	$\lambda_p = 2.26\sqrt{\frac{E_a}{f_y}}$ $\lambda_p = 65.93\varepsilon$	$N_{AISC} = N_0 0.658^{\frac{N_0}{N_{cr}}}$ $N_0 = A_s \cdot f_y + \alpha \cdot A_c \cdot f_{ck}$ $\alpha_{circular} = 0.95$	$\alpha_{rectangular} = 0.85$
DBJ [20]	$235 \le f_y \le 420$ $E_a = 206GPa$	$30 \le f_{cu}^{150} \le 90$ $E_c = \frac{10^5}{2.2 + \frac{34.7}{\rho}}$	$\frac{D}{t} \le 150\frac{235}{f_y}$ $\frac{D}{t} \le 150\varepsilon^2$	$\frac{H}{t} \le 60\sqrt{\frac{235}{f_y}}$ $\frac{H}{t} \le 60\varepsilon$	$N_{DBJ} = f_{sc}(A_s + A_c)$ $\xi_0 = \frac{A_s \cdot f_y}{A_c \cdot f_{ck}}$ $f_{sc,circular} = (1.14 + 1.02\xi_0) f_{ck}$	$f_{sc,rect} = (1.18 + 0.85\xi_0) f_{ck}$
AS [21]	$f_y \le 450$ $E_a = 200GPa$	$25 \le f_{ck} \le 65$ $E_c = 0.043\rho^{1.5}\sqrt{f_{ck}}$	$\frac{D}{t}\sqrt{\frac{f_y}{250}} \le 82$ $\frac{D}{t} \le 87.23\varepsilon^2$	$\frac{H}{t}\cdot\sqrt{\frac{f_y}{250}} \le$ $\le \begin{cases} 45 & \text{hot} \\ 40 & \text{cold} \\ 35 & \text{welded} \end{cases}$	$N_{AS} = \eta_a A_a f_y + \left(1 + \eta_c \frac{t}{D}\frac{f_y}{f_{ck}}\right) A_c f_{ck}$ $\eta_a = 0.25(3 + 2\bar{\lambda}) \le 1$ $\eta_c = 4.9 - 18.5\bar{\lambda} + 17\bar{\lambda}^2 \ge 0$	$N_{AS} = A_s f_y + A_c f_{ck}$

LIST OF FIGURE CAPTIONS

LIST OF TABLE CAPTIONS